Superconductor-to-insulator transition in boron-doped diamond films grown using chemical vapor deposition

Akihiro Kawano,[1] Hitoshi Ishiwata,[1] Shingo Iriyama,[1] Ryosuke Okada,[1] Takahide Yamaguchi,[2] Yoshihiko Takano,[2] and Hiroshi Kawarada[1]

[1]*School of Science and Engineering, Waseda University, 3-4-1 Okubo, Shinjuku, Tokyo 169-8555, Japan*

[2]*National Institute for Materials Science, 1-2-1 Sengen, Tsukuba 305-0047, Japan*

(Received 29 May 2010; published 16 August 2010)

The critical concentration of superconductor-to-insulator transition in boron-doped diamond is determined in two ways, namely, the actual doping concentration of boron and the Hall carrier concentration. Hall carrier concentrations in (111) and (001) films exceed the actual doping concentration owing to the distortion of the Fermi surface. The high critical boron concentration in (110) films is owing to the effect of the high concentration of interstitial boron atoms. A boron concentration of 3×10^{20} cm^{-3} in substitutional site is required for inducing superconductivity in diamond.

DOI: 10.1103/PhysRevB.82.085318 PACS number(s): 71.55.Cn, 74.78.−w, 74.25.Dw, 74.62.Dh

I. INTRODUCTION

The discovery of superconductivity in a degenerate semiconductor of boron-doped diamond in 2004 (Refs. 1–3) stimulated the studies of the low-carrier-density superconductor of a doped semiconductor. The observations of superconductivity have been reported subsequently in other doped semiconductors, namely, silicon,[4] silicon carbide,[5] and recently germanium.[6] The superconducting transition temperature (T_C) in boron-doped diamond is high among such doped semiconductors.[7,8] The zero-resistivity temperature $T_{C\ offset}$ in (111) films is 7.4 K with the actual doping concentration $n_B=8\times10^{21}$ cm^{-3}. T_C depends on the growth orientation. $T_{C\ offset}$ in (001) films is 3.2 K despite the same boron concentration. To provide an insight into the research of superconductivity in the doped semiconductor, the quantitative data about the doping dependence of T_C is investigated in the wide boron concentration range of $1\times10^{20}<n_B<1\times10^{22}$ cm^{-3}, considering growth orientations, such as (111), (001), and (110). Moreover, both the boron concentration n_B measured by secondary ion mass spectroscopy (SIMS) and the effective carrier concentration n_H measured by Hall effect measurement are evaluated. The ratio of boron concentration n_B and carrier concentration n_H reveals the superconductor-to-insulator (SI) transition in boron-doped diamond more clearly.

II. SAMPLE PREPARATION AND EXPERIMENTS

All boron-doped diamond films were epitaxially grown by quartz tube-type microwave plasma-assisted chemical vapor deposition (CVD). (111), (001), and (110) single-crystalline diamond substrates synthesized under high pressure and high temperature were employed. The thicknesses of the samples are above 100 nm, from which we have confirmed that T_C is not affected by the sample thickness. To distinguish between a superconductor and an insulator clearly, the superconducting transition temperature was defined as the temperature at which resistivity decreases to 90% of the normal-state resistivity. Actual doping concentrations of boron n_B in the films were measured by SIMS. Carrier concentrations n_H were measured by Hall effect measurement in the magnetic field range of ±5 T at 300 K. n_H is given by $n_H=1/(eR_H)=I_xB/etV_H$, assuming that the Fermi surface is simply spherical. Here, R_H is the Hall coefficient, I_x is the current through the sample, t is the film thickness, and V_H is the Hall voltage. X-ray diffraction (XRD) was performed to evaluate the crystalline lattice expansion of boron-doped diamond films. θ-2θ curves of (111), (004), and (220) symmetric Bragg reflections were measured in (111), (001), and (110) films, respectively. Reciprocal space mapping (RSM) of (113) asymmetric Bragg reflections was also performed to evaluate both perpendicular and in-plane lattice expansions in (111) and (001) films. The uncertainty of n_B, n_H and lattice expansion ratio is minimized by using large samples of 2–3 mm. The distribution of boron atoms measured by SIMS is homogenous.[9] Total errors are less than 40%.

III. DOPING CONCENTRATION AND SUPERCONDUCTIVITY

The dependence of T_C on the boron concentration n_B measured by SIMS is shown in Fig. 1. For $n_B<3\times10^{20}$ cm^{-3} in (111) films, the samples do not show the superconducting transition down to 0.4 K. The sharp drops in resistivity are clearly observed above that concentration. The critical boron concentration of SI transition in (111) films is estimated to be 3×10^{20} cm^{-3}. T_C in (111) films does not tend to saturate up to the maximum T_C of 8.3 K with $n_B=8\times10^{21}$ cm^{-3}. T_C in (001) films is almost the same as that in (111) films around SI transition. The critical boron concentration in (001) films is estimated to be 3×10^{20} cm^{-3}. T_C in (001) films seems to saturate, unlike that in (111) films. The superconducting transition in (111) and (001) films occurs in the concentration range of $3\times10^{20}<n_B<1\times10^{22}$ cm^{-3}, which is a very wide compared with other superconductors ($9\times10^{18}<n_B<3\times10^{20}$ cm^{-3} in $SrTiO_3$ and $6\times10^{20}<n_B<2\times10^{21}$ cm^{-3} in $La_{2-x}Sr_xCuO_4$). Considering the very wide concentration range, the maximum $T_C=8.3$ K may be the optimum. However, the optimum concentration has not been estimated because the boron cannot

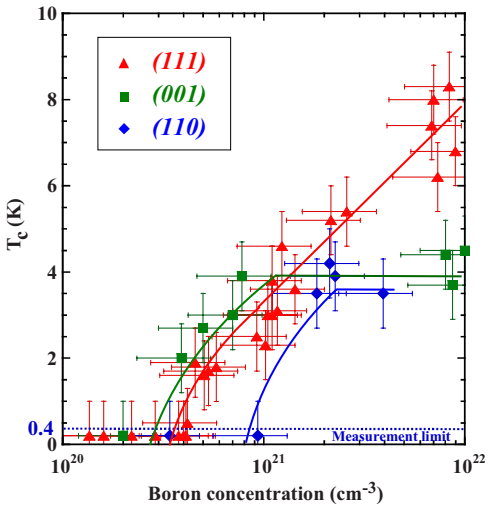

FIG. 1. (Color online) Dependence of T_C on boron concentration measured by SIMS. Triangle plots are for (111) boron-doped diamond films, square plots for (001) films, and diamond-shaped plots for (110) films. Solid lines are drawn so as to fit the data in the plots. The dashed line shows the measurement limit of the temperature (0.4 K) in our ^{3}He cooling system. The critical boron concentrations of superconductor-to-insulator transition are estimated to be 3×10^{20} cm^{-3} in (111) and (001) films and 9×10^{20} cm^{-3} in (110) films.

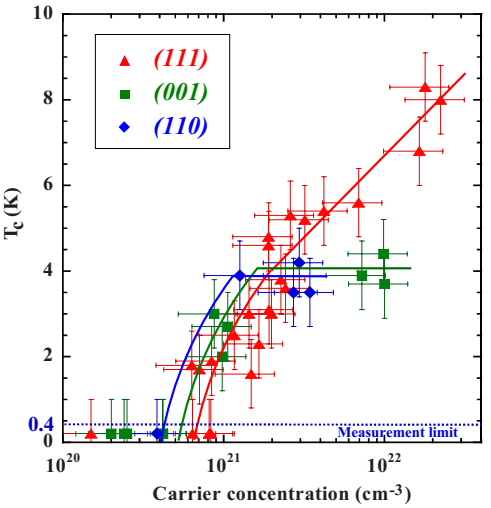

FIG. 2. (Color online) Dependence of T_C on carrier concentration estimated by Hall effect measurement. Triangle plots are for (111) boron-doped diamond films, square plots for (001) films, and diamond-shaped plots for (110) films. Solid lines are drawn so as to fit the data in plots. All of the solid lines approach 4×10^{20} cm^{-3} at zero temperature. The critical carrier concentrations of superconductor-to-insulator transition are estimated to be 4×10^{20} cm^{-3}.

be incorporated above 1×10^{22} cm^{-3} in the present doping technology. Some theoretical studies predict the higher T_C with increasing the doping concentration. The superconducting properties in (110) films are also evaluated. It is difficult to incorporate boron atoms into (110) films. The maximum doping level in (110) films is 4×10^{21} cm^{-3} which is twice lower than those in (111) and (001) films. Superconductivity is not observed for $n_B<9\times10^{20}$ cm^{-3} for (110) films. The critical boron concentration of SI transition in (110) films is 9×10^{20} cm^{-3} which is very different from those in (111) and (001) films.

On the other hand, the relationship between T_C and the carrier concentration n_H $(=1/eR_H)$ measured by Hall effect measurement on the basis of the simple assumption exhibits a different behavior, as shown in Fig. 2. T_C as a function of carrier concentration n_H is almost the same around SI transition, independent of the growth orientation. The critical carrier concentration of SI transition is 4×10^{20} cm^{-3}. The carrier concentration in (110) films is generally lower than boron concentration. The critical boron concentration of 9×10^{20} cm^{-3} in (110) films is much higher than the critical carrier concentration of 4×10^{20} cm^{-3}. In contrast, the critical boron concentration of 3×10^{20} cm^{-3} in (111) and (001) films is lower than the critical carrier concentration.

Figure 3 shows the relationship between the carrier and boron concentrations. The Hall carrier concentration exceeds the actual doping concentration for $n_B\gtrsim3\times10^{20}$ cm^{-3} in (111) and (001) films except one (001) sample. Only in the superconducting sample, anomaly high carrier concentration is observed. Hall carrier concentration n_H deviates from the actual doping concentration n_B by the Hall scattering factor r_H according to

$$n_B = r_H \cdot n_H = \frac{r_H}{eR_H}. \quad (1)$$

r_H is calculated by the ratio between n_B and n_H. In this work, r_H of (111) and (001) heavily boron-doped diamond is 0.2–1.0 for assuming that all dopants are activated. The Hall

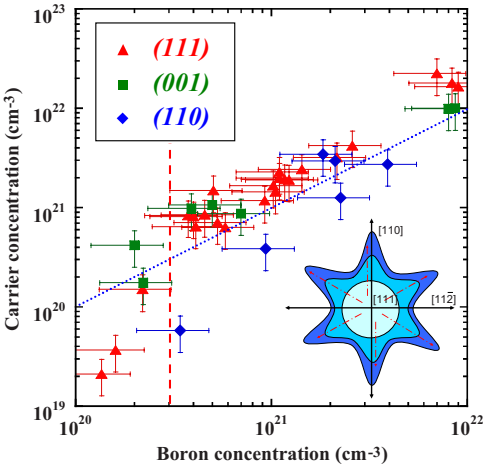

FIG. 3. (Color online) Relationship between carrier concentration n_H and boron concentration n_B in (111) films. The dotted line is a fit to $n_H/n_B=1$ (one carrier per boron atom). The dashed line shows the critical boron concentration of superconductor-to-insulator transition in (111) and (001) films $(=3\times10^{20}$ cm$^{-3})$. The carrier concentration exceeds the boron concentration for $n_B\gtrsim3\times10^{20}$ cm^{-3}. In contrast, the carrier concentration is the below boron concentration for $n_B\lesssim3\times10^{20}$ cm^{-3}. Inset is a schematic of the Fermi surface in the (111) plane of $\boldsymbol{k}$ space. The Fermi surface extends along the {110} directions.

scattering factor is determined as $r_H=\langle\tau^2\rangle/\langle\tau\rangle^2$, where τ is the relaxation time of the carrier.[10] Then, r_H is related to the scattering mechanism and the band structure. For nondegenerate and spherically symmetric band structure, $r_H>1$ is given. As it is well known, $r_H=3\pi/8=1.18$ for phonon scattering and $r_H=315\pi/512=1.93$ for ionized impurity scattering in the case of the nondegenerate single band. However, Allgaier[11] indicated that anisotropy of the Fermi surface decreases r_H and induces $r_H<1$. Carrier concentration exceeds actual doping concentration due to the distorted Fermi surface. The top of the valence band in diamond (including other diamond structure such as silicon and germanium) at the Γ point is triply degenerate. When the Fermi level (E_F) enters into the valence band and the bands move away from Γ point, the three bands split and become anisotropic, as calculated by Cardona[12] and Boeri *et al.*[13] A schematic of the Fermi surface in the (111) plane of $\boldsymbol{k}$ space is shown in the inset of Fig. 3. The Fermi surface extends along the {110} directions in heavily boron-doped diamond. This distorted Fermi surface in the valence band causes $r_H<1$, as is also indicated in silicon[14,15] and germanium.[16] Yokoya[17] evaluated the band structure with angle-resolved photoemission spectroscopy in our (111) boron-doped CVD diamond samples. For $n_B=3\times10^{20}$ cm^{-3}, the E_F lies around the top of the valence band. In the heavily doped region, the E_F enters the valence band. The boron concentration has an important effect on the position of E_F from the valence-band maximum and superconducting properties. Unlike in silicon and germanium, the metal-insulator transition (MIT) in diamond is not related to the Mott's conventional MIT. When the E_F enters into the valence band, the system becomes metallic. The boron concentration of SI transition corresponds to that of MIT. Intermediate concentration region (metal, but not superconductivity) does not exist. In insulating region, the hopping conductivity is observed as also reported by Klein *et al.*[18]

It is generally observed in superconductor metals that Hall carrier concentration exceeds atomic concentration.[19,20] In some cases, Hall carrier concentration of superconductor metals is several times larger than that of nonsuperconductor metals. The reason for this is that the Fermi surface is not simply spherical. The Fermi surface of superconductor metals is distorted compared with that of nonsuperconductor metals. The distorted Fermi surface results in large Hall concentration and superconducting transition. It is worth noting that the Hall mobility μ_H of boron-doped diamond with $n_B \gtrsim 3\times10^{20}$ cm^{-3} is 1–10 cm^2/V s and close to those of typical superconductor metals. For example, μ_H of Pb is 8.4.[20]

IV. LATTICE EXPANSION

The critical boron concentration of SI transition is different among three growth orientation as shown in Fig. 1. On the other hand, the critical carrier concentration of SI transition is same independent of the growth orientation as shown in Fig. 2. This fact leads us to understand that the doping site is related to superconductivity in diamond. The perpendicular lattice expansion measured by XRD as a function of boron concentration is shown in Fig. 4. Vegard's law is the model representing the lattice mismatch when the dopant occupies the substitutional site.[21] Vegard's law in boron-doped diamond is expressed as

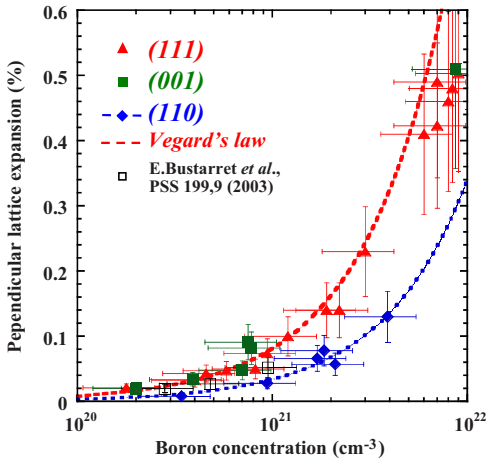

FIG. 4. (Color online) Perpendicular lattice expansion as a function of boron concentration: triangle plots are for (111) boron-doped diamond films, square plots for (001) films, and diamond-shaped plots for (110) films. Open square plots are reported by Bustarret *et al.* Dashed line shows the Vegard's law using the covalent bonding radii r_B and r_C of 0.088 nm and 0.077 nm, respectively. Dotted line is drawn so as to fit the data in plots of (110) films.

$$\frac{\Delta a}{a_s}=\frac{r_B-r_C}{r_C}\frac{n_B}{n_C}=8.12\times10^{-25}\cdot n_B, \tag{2}$$

where $\Delta a/a_s$ is the lattice expansion ratio. a_s is the lattice constant of the substrate and 3.5671 Å in diamond. r_B and r_C are covalent bonding radii of boron and carbon atoms, namely, 0.088 nm and 0.077 nm, respectively. n_C is the concentration of carbon atoms. The perpendicular lattice expansions in (111) and (001) films fit Vegard's law. It is deduced that almost all the boron atoms occupy the substitutional site in (111) and (001) films and fully activated. An additional contribution of the deformation potential should be considered. The free carrier concentration shifts the energies of the valence- and conduction-band maximums. The change in the total energy of the semiconductor shifts the lattice parameter. Bardeen and Shockley[22] proposed and Yokota[23] introduced an additional term to the Vegard's law in p-type semiconductors. It can be deduced from the results in (111) and (001) films that the contribution of the deformation potential is small compared with that of the introduction of substitutional boron. Thus, the amount of substitutional boron atoms mainly determines the lattice expansion.

On the other hand, the lattice expansion ratios in (110) films are far lower than the theoretical values. As the interstitial dopant atoms increase, the lattice mismatch deviates downward from Vegard's law. Therefore, it is predicted that (110) films have a high interstitial boron concentration. Around the critical boron concentration of 9×10^{20} cm^{-3} in (110) films, only the boron concentration of 3×10^{20} cm^{-3} may occupy substitutional site and contribute carriers related to the superconducting transition. The first work for the SI

transition by Bustarret *et al.*[3] and Klein *et al.*[18] can also be explained from the amount of interstitial boron atoms. The critical boron concentration of their (001) CVD samples fabricated using a $H_2/CH_4/B_2H_6$ gas mixture was 5×10^{20} cm^{-3}, which is higher than that of 3×10^{20} cm^{-3} in our (111) and (001) films. The lattice expansions in their works are smaller than those in our (111) and (001) films as shown in Fig. 4.[24] It is indicated that the samples reported by Bustarret *et al.* and Klein *et al.* have a high concentration of interstitial boron atoms compared with our (111) and (001) films. Other possible contribution to the lattice expansion is B-B dimers. However, the B-B bond length is very large. The existence of B-B dimers induces upward deviations in the diamond lattice.[25] In the case of (110) films, B-B dimers do not contribute deviations from Vegard's law.

Figure 5(a) shows the dependence of T_C on the perpendicular lattice expansion ratio deduced by x-ray diffraction. The T_C dependence is the same except for the heavy concentration range. This indicates that only substitutional boron induces superconductivity. The lattice expansion ratios approach 0.25% as T_C approaches zero, which corresponds to the situation where the diamond lattice has a boron concentration of 3×10^{20} cm^{-3}. The difference of T_C between (111) and (001) films in the heavy doping range is explained by the shape of lattice expansion. Figure 5(b) shows the dependence of T_C on the in-plane lattice expansion ratio. Insets are the shape of the lattice expansion of (111) and (001) samples. In (111) samples, in-plane lattice fit the substrate. The crystalline lattice is strained like a heteroepitaxial growth such as SiGe on Si. In-plane lattice expansion ratio is less than 0.08% of the measurement limit of RSM with XRD. On the other hand, a relaxed and isotropic layer exists in (001) samples. Note that the Vegard's law for the strained layer is different from Eq. (2) by $1+\nu/1-\nu$, where ν is Poisson's ratio.[26] However, Poisson's ratio of diamond is 0.08 which is much smaller than other materials. The calculated values of Vegard's law for the strained and relaxed and layer is different by a factor of 1.18. The number is less than the errors of the measurement. The lattice strain changes the Fermi-surface toporogy and then r_H.[27] In the heavily doped region of $n_B \sim 1 \times 10^{22}$ cm^{-3}, carrier concentration in (111) films is larger than that in (001) films. r_H is 0.3–0.5 in (111) films while r_H is 0.7–0.8 in (001) films. This difference may be attributed to the crystalline lattice strain.

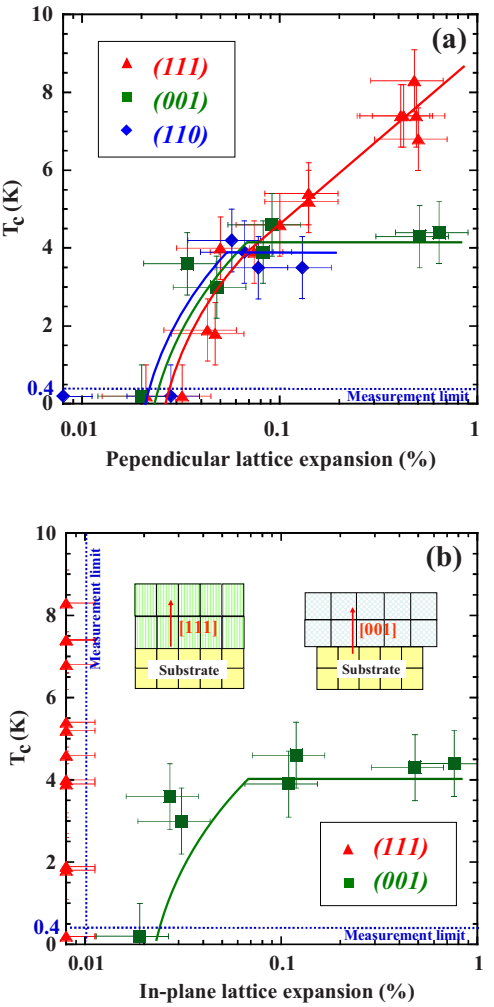

FIG. 5. (Color online) Dependence of T_C on (a) perpendicular and (b) in-plane lattice expansion ratio deduced by x-ray diffraction. Triangle plots are for (111) boron-doped diamond films, square plots for (001) films, and diamond-shaped plots for (110) films. Solid lines are drawn so as to fit the data in plots. Insets are the shape of the lattice expansion of (111) and (001) samples.

V. CONCLUSION

The critical boron concentration of superconductor-to-insulator transition in (111) and (001) films is 3×10^{20} cm^{-3}, which is different from that of 9×10^{20} cm^{-3} in (110) films. On the other hand, the critical carrier concentration evaluated by Hall effect measurement is a common value (4×10^{20} cm^{-3}) in the three orientations. Carrier concentration is also a valuable parameter in diamond superconductor. The high critical boron concentration in (110) films is due to the existence of interstitial boron atoms. A boron concentration of 3×10^{20} cm^{-3} in substitutional site is required for inducing superconductivity in diamond. Carrier concentrations in (111) and (001) films exceed the actual doping concentration in superconducting region. One of the major reasons is caused by the distortion of the Fermi surface.

ACKNOWLEDGMENT

This research was partially supported by the Ministry of Education, Culture, Sports, Science and Technology, Japan, a Grant-in-Aid for Scientific Research S (Grant No. 19106006).

[1] E. A. Ekimov, V. A. Sidrov, E. D. Bauer, N. N. Mel'nik, N. J. Curro, J. D. Thompson, and S. M. Stishov, Nature (London) **428**, 542 (2004).
[2] Y. Takano, M. Nagao, I. Sakaguhci, and M. Tachiki, T, Hatano, K. Kobayashi, H. Umezawa, and H. Kawarada, Appl. Phys. Lett. **85**, 2851 (2004).
[3] E. Bustarret, J. Kaĉmarĉik, C. Marcenat, E. Gheeraert, C. Cytermann, J. Marcus, and T. Klein, Phys. Rev. Lett. **93**, 237005 (2004).
[4] E. Bustarret, C. Marcenat, P. Achatz, J. Kaĉmarĉik, F. Lévy, A. Huxley, L. Ortéga, E. Bourgeois, X. Blase, D. Débarre, and J. Boulmer, Nature (London) **444**, 465 (2006).
[5] Z.-A. Ren, J. Kato, T. Muranaka, J. Akimitsu, M. Kriener, and Y. Maeno, J. Phys. Soc. Jpn. **76**, 103710 (2007).
[6] T. Herrmannsdörfer, V. Heera, O. Ignatchik, M. Uhlarz, A. Mücklich, M. Posselt, H. Reuther, B. Schmidt, K.-H. Heinig, W. Skorupa, M. Voelskow, C. Wündisch, R. Skrotzki, M. Helm, and J. Wosnitza, Phys. Rev. Lett. **102**, 217003 (2009).
[7] H. Umezawa, T. Takenouchi, Y. Takano, K. Kobayashi, M. Nagao, I. Sakaguchi, M. Tachiki, T. Hatano, G. Zhong, M. Tachiki, and H. Kawarada, arXiv:cond-mat/0503303 (unpublished).
[8] Y. Takano, J. Phys.: Condens. Matter **21**, 253201 (2009).
[9] A. Kawano, H. Ishiwata, S. Iriyama, R. Okada, S. Kitagoh, M. Watanabe, Y. Takano, T. Yamaguchi, and H. Kawarada, Physica C (to be published).
[10] R. A. Smith, *Semiconductors* (Cambridge University Press, Cambrdge, 1978) pp. 122–125.
[11] R. S. Allgaier, Phys. Rev. **165**, 775 (1968).
[12] M. Cardona, Sci. Technol. Adv. Mater. **7**, S60 (2006).
[13] L. Boeri, J. Kortus, and O. K. Anderson, J. Phys. Chem. Solids **67**, 552 (2006).
[14] F. Szmulowicz, Appl. Phys. Lett. **43**, 485 (1983).
[15] F. Szmulowicz, Phys. Rev. B **34**, 4031 (1986).
[16] W. Bernard, Phys. Rev. **132**, 33 (1963).
[17] T. Yokoya, T. Nakamura, T. Matsushita, T. Muro, Y. Takano, M. Nagao, T. Takenouchi, H. Kawarada, and T. Oguchi, Nature (London) **438**, 647 (2005).
[18] T. Klein, P. Achatz, J. Kacmarcik, C. Marcenat, F. Gustafsson, J. Marcus, E. Bustarret, J. Pernot, F. Omnes, B. E. Sernelius, C. Persson, A. Ferreira da Silva, and C. Cytermann, Phys. Rev. B **75**, 165313 (2007).
[19] S. Fujita and S. Godoy, in *Quantum Statistical Theory of Superconductivity*, edited by S. Wolf (Plenum Press, New York, London, 1996), pp. 83–99.
[20] I. Kikoin and B. Lasarew, Nature (London) **129**, 57 (1932).
[21] L. Vegard, Z. Phys. **5**, 17 (1921).
[22] J. Bardeen and W. Shockley, Phys. Rev. **80**, 72 (1950).
[23] I. Yokota, J. Phys. Soc. Jpn. **19**, 1487 (1964).
[24] E. Bustarret, E. Gheeraert, and K. Watanabe, Phys. Status Solidi A **199**, 9 (2003).
[25] J. E. Moussa and M. L. Cohen, Phys. Rev. B **77**, 064518 (2008).
[26] C. A. Klein and G. F. Cardinale, Diamond Relat. Mater. **2**, 918 (1993).
[27] J. E. Dijkstra and W. Th. Wenckebach, J. Appl. Phys. **85**, 1587 (1999).